D. O. (1986) *Endocrinology (Baltimore) 119*, 1549–1557.
Towbin, H., Staehelin, T., & Gordon, J. (1979) *Proc. Natl. Acad. Sci. U.S.A. 76*, 4350–4354.
Tuohimaa, P., Renoir, J.-M., Radanyi, C., Mester, J., Joab, I., Buchou, T., & Baulieu, E.-E. (1984) *Biochem. Biophys. Res. Commun. 119*, 433–439.
von der Ahe, D., Janick, S., Scheidereit, C., Renkawitz, R., Schütz, G., & Beato, M. (1985) *Nature (London) 313*, 706–709.
von der Ahe, D., Renoir, J. M., Buchou, T., Baulieu, E.-E., & Beato, M. (1986) *Proc. Natl. Acad. Sci. U.S.A. 83*, 2817–2821.
Wegener, A. D., & Jones, L. R. (1984) *J. Biol. Chem. 259*, 1834–1841.
Welch, W. J., Garrels, J., Thomas, G. O., Lin, J. J.-C., & Feramisco, J. R. (1983) *J. Biol. Chem. 258*, 7102–7111.
Wileman, T., Harding, C., & Stahl, P. (1985) *Biochem. J. 232*, 1–14.
Wrange, O., Okret, S., Radojcic, M., Carlstedt-Duke, J., & Gustafsson, J.-A. (1984) *J. Biol. Chem. 259*, 4534–4541.

Distributions of Fluorescence Decay Times for Parinaric Acids in Phospholipid Membranes†

D. R. James, J. R. Turnbull, B. D. Wagner, W. R. Ware, and N. O. Petersen*
Photochemistry Unit, Department of Chemistry, The University of Western Ontario, London, Ontario, Canada N6A 5B7
Received August 19, 1986; Revised Manuscript Received May 4, 1987

ABSTRACT: Analysis of fluorescence decay data for probes incorporated into model or biological membranes invariably requires fitting to more than one decay time even though the same probe exhibits nearly single-exponential decay in solution. The parinaric acids (cis and trans) are examples of this. Data are presented for both parinaric acid isomers in dimyristoylphosphatidylcholine membranes collected to higher precision than normally encountered, and the fluorescence decays are shown to be best described by a smooth *distribution* of decay times rather than by a few discrete lifetimes. The temperature dependence of the fluorescence decay reveals a clear shift in the distribution to longer lifetimes associated with the membrane phase transition at 23.5 °C. The physical significance is that fluorescence lifetime measurements appear to reflect a physical process with a distribution of lifetimes rather than several distinct physical processes.

Fluorescence spectroscopy provides a convenient, sensitive, and selective tool for studying dynamic processes in biological membranes (Yguerabide & Foster, 1981; Devaux & Seigneuret, 1985). Fluorescence lifetime measurements are of intrinsic interest but are also essential to adequately interpret temperature- and concentration-dependent quantum yield changes and form the bases for correct analysis of both steady-state and time-resolved fluorescence anisotropy data. As the application of fluorescence techniques to membrane research has developed, the complexity of the data analysis and interpretation in terms of physical processes has steadily increased. The development of diphenylhexatriene as a probe of membrane disorder is a prime example (Chen et al., 1977; Kawato et al., 1977; Lakowicz et al., 1985).

Fluorescence decay data obtained from probes in membranes invariably must be analyzed by fits to two or more exponential decays, frequently with decay times differing by less than a factor of 2 or 3 (Blatt & Sawyer, 1985; Devaux & Seigneuret, 1985; Petersen et al., 1987; Vincent & Gallay, 1984; Wolber & Hudson, 1981). This is a perplexing and poorly understood feature of these systems, particularly since most of the probes exhibit nearly single-exponential decays in homogeneous solution (Wolber & Hudson, 1981; Vincent & Gallay, 1984; Parasassi et al., 1984). In many cases the set of lifetimes (two or three) has been attributed to compartmentalization of the probes in different membrane environments, and the proportion of each component has been related to the probe concentration in each environment (Devaux & Seigneuret, 1985; Klausner et al., 1980; Karnovsky et al., 1982). In a few cases it has been suggested that the set of lifetimes may arise from a distribution of lifetimes, but no evidence was presented (Petersen et al., 1987; Wolber & Hudson, 1981).

Recently James and Ware (1985, 1986) have demonstrated through extensive computer simulations that with fluorescence decay data at normal levels of precision (20 000–50 000 counts in the peak channel) it is impossible to distinguish between two or three discrete lifetimes and a continuous distribution of lifetimes by any criteria of goodness of fits. However, as the precision of the data increases (to 200 000 counts in the peak channel or more), it becomes possible to recover the true distribution of lifetimes, whether it is unimodal or bimodal or contains discrete lifetimes (James & Ware, 1986).

In this paper we apply the methods of James and Ware (1986) to the analysis of fluorescence decay curves collected to high precision for both *cis*- and *trans*-parinaric acid in dimyristoylphosphatidylcholine (DMPC)[1] membranes and show that in both cases smooth distributions of decay times are recovered. Analysis of measurements performed as a function of increasing temperature through the main phase

† Contribution No. 337. This work is supported by NSERC Canada and the Academic Development Fund of The University of Western Ontario. J.R.T. was a Summer Undergraduate Research Fellow (NSERC).

[1] Abbreviations: t-PnA, *trans*-parinaric acid; c-PnA, *cis*-parinaric acid; DMPC, dimyristoylphosphatidylcholine; ESM, exponential series method; n-AS, *n*-(9-anthroyloxy)stearic acid; POPC, palmitoyloleoylphosphatidylcholine; CPC, counts in peak channel.

0006-2960/87/0426-6272$01.50/0

transition shows that the distribution of lifetimes shifts cleanly to another distribution centered at shorter lifetimes. Although this analysis of decay data in terms of lifetime distributions requires better data and is more complex, it is necessary if one wants to understand the dynamic processes of the probes in membranes. At this time it appears that the physical picture which emerges is simpler and easier to rationalize for the anisotropic membrane environment than models based on two, three, or four exponentials.

Materials and Methods

The *cis*- and *trans*-parinaric acids (Molecular Probes, Inc.) and DMPC (Sigma) were used without further purification. 3-Methylindole (Aldrich) was purified by successive recrystallization from water. Stock solutions of the parinaric acids and the lipid in absolute ethanol were stored at −20 °C after degassing and were used within a few days of preparation. Membranes were prepared by mixing appropriate amounts of the stock solutions into a total of 60 μL of ethanol, which was subsequently injected into 5 mL of warm (45–50 °C) vigorously stirred phosphate-buffered saline solution (pH 7.4; GIBCO). This procedure produces unilamellar vesicles (Fung & Stryer, 1978). The samples all contained 8×10^{-4} M DMPC and 8×10^{-7} M parinaric acid.

Fluorescence decay data were acquired by using the time-correlated single photon counting technique. The excitation source was the frequency-doubled output from a rhodamine 6G dye laser (Coherent 590) pumped by a mode-locked argon ion laser (Coherent CR-8 with an Innova tube). Pulses of light at 580 nm and of about 10-ps duration were removed from the dye laser with a cavity dumper (Coherent 7200) operating at 1 MHz. The excitation wavelength of 290 nm lies well within the absorption band of the parinaric acids but is not at the maximal absorption (Sklar et al., 1977).

Fluorescence emission was monitored at right angles through a cutoff filter (to attenuate the scattered light) and with a magic angle polarizer (to minimize depolarization artifacts). The sample temperature was controlled and monitored to better than 0.1 °C. Further details of the picosecond lifetime apparatus have been published (Ware et al., 1983).

Fluorescence decay data were collected for solutions of 3-methylindole in water with various amounts of HCl in order to produce a set of single-exponential decay curves at particular lifetimes. Composite decay curves were constructed from these real data to simulate the decay curves one would observe from a system characterized by a set of discrete lifetimes.

Artificial decay data were constructed by adding up to 112 individual, computer-generated single-exponential decay curves. The curves were weighted to simulate decay curves characteristic of a continuous distribution of lifetimes, and Poisson noise was added to simulate the appropriate data precision.

The data were analyzed either by a freely adjustable multiexponential analysis method using up to four exponentials, i.e., up to eight parameters, or by the exponential series method described in detail by James and Ware (1986). Both methods assume that the fluorescence decay, $D(t)$, can be analyzed as a sum of exponentials as in eq 1. The multiexponential

$$D(t) = \sum_{m=1}^{N} a_m \exp[-t/\tau_m] \quad (1)$$

analysis method typically uses N less than or equal to four, and the recovered lifetimes, τ_m, and their associated preexponential factors, a_m, are usually considered to arise from discrete emitting states or species (in the absence of interconversion among species in the excited state). The exponential series method treats eq 1 as a discrete approximation to

$$D(t) = \int_0^\infty A(\tau) \exp(-t/\tau)\, d\tau \quad (2)$$

and uses N greater than 20 for fixed lifetime values. Here $A(\tau)$ is the continuous fluorescence lifetime distribution causing the observed decay. Thus the preexponential values recovered from the fit represent an approximation to $A(\tau)$. In both cases the experimental data consist of a convolved decay curve, and the trial recovery curve, $D(t)$, is obtained by iterative reconvolution with the instrumental response function.

The exponential series method uses a fixed set of lifetimes and fits to freely adjustable a_m values that are constrained to be positive. The search for the best fit uses the Marquardt algorithm to minimize the reduced χ^2. If, during the iterative minimization process, a preexponential value falls below 1% of the currently maximal a_m, that preexponential value is fixed at zero to facilitate convergence. Through numerous simulations, the exponential series method has been shown to reliably recover a wide range of distributions, including the limiting case of a discrete set of lifetimes. In particular, we have found and we will show that the method can successfully recover distributions similar to those presented in this work and can discriminate against the alternative discrete set of lifetimes extracted by multiexponential analyses.

Results and Discussion

Figure 1 shows the results of a multiexponential analysis of the fluorescence decay of *cis*-parinaric acid in DMPC at 15 °C with data containing either 2×10^4 or 2×10^5 counts in the peak channel. As illustrated in Figure 1b, the decay is adequately described by three exponentials at the lower levels of precision as judged by the random pattern of the residuals. However, at the higher levels of precision, neither three nor four exponentials are sufficient to remove the low-frequency, nonrandom pattern in the residuals (Figure 1c,d). These fits of the high-precision data suggest that a discrete multiexponential analysis is inadequate and that a more complete analysis for the distribution may be appropriate.

A high-frequency pattern of oscillation suggestive of radio frequency (RF) pickup is evident in the residuals of the high-precision data (Figures 1c,d). At high count levels this systematic noise is greater than the characteristic Poisson statistical noise arising from the time-correlated single photon counting technique. The source of this RF noise is unknown, but its presence limits the precision of the fit. Fortunately, the RF noise does not appear to alter the quality of the fits or introduce artificial lifetime components, which would appear at short time. Nevertheless, the systematic noise increases the value of χ^2 significantly above unity even when the residuals and the autocorrelation functions appear "random" (Figure 1) (James et al., unpublished results). The contribution of this and other potential artifacts is discussed further below.

Figure 2a shows the distribution of lifetimes recovered by applying the exponential series method to the high-precision data for both parinaric acids at 15 °C. The bars in the figure are the results recovered from the four exponential fits to the same data.

Figure 2b shows a comparison of the residuals from the two fits to the *cis*-parinaric acid. The residual patterns are quite similar and do not provide an adequate tool for deciding which is the better fit. We must, therefore, assess whether the exponential series method can differentiate discrete lifetimes from a distribution of lifetimes.

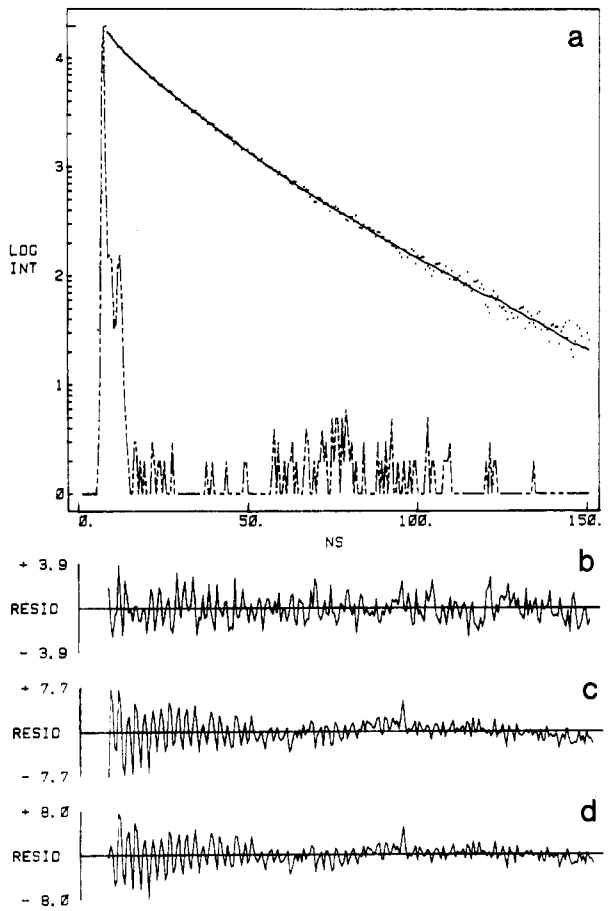

FIGURE 1: Fluorescence decay of *cis*-parinaric acid in DMPC vesicles. (a) Decay curve at 2×10^4 counts in the peak channel (CPC): (---) instrument response function; (···) decay raw data; (—) fitted curve. Time is plotted on the x axis, and the logarithm of the intensity is plotted on the y axis. (b) Weighted residuals of the fit at 2×10^4 CPC to a three-exponential decay: $a_1 = 0.274$, $\tau_1 = 3.22$ ns; $a_2 = 0.383$, $\tau_2 = 13.0$ ns; $a_3 = 0.343$, $\tau_3 = 22.8$ ns; $\chi^2 = 1.503$. (c) Weighted residuals of the fit at 2×10^5 CPC to a three-exponential decay: $a_1 = 0.282$, $\tau_1 = 2.79$ ns; $a_2 = 0.421$, $\tau_2 = 12.9$ ns; $a_3 = 0.297$, $\tau_3 = 23.8$ ns; $\chi^2 = 5.13$. (d) Weighted residuals of the fit at 2×10^5 CPC to a four-exponential decay: $a_1 = 0.494$, $\tau_1 = 0.35$ ns; $a_2 = 0.144$, $\tau_2 = 4.04$ ns; $a_3 = 0.25$, $\tau_3 = 15.0$ ns; $a_4 = 0.112$, $\tau_4 = 25.5$ ns; $\chi^2 = 4.51$. As noted in the text, the χ^2 at 2×10^5 is higher than expected. Uncertainties in the numbers quoted are in the last digit.

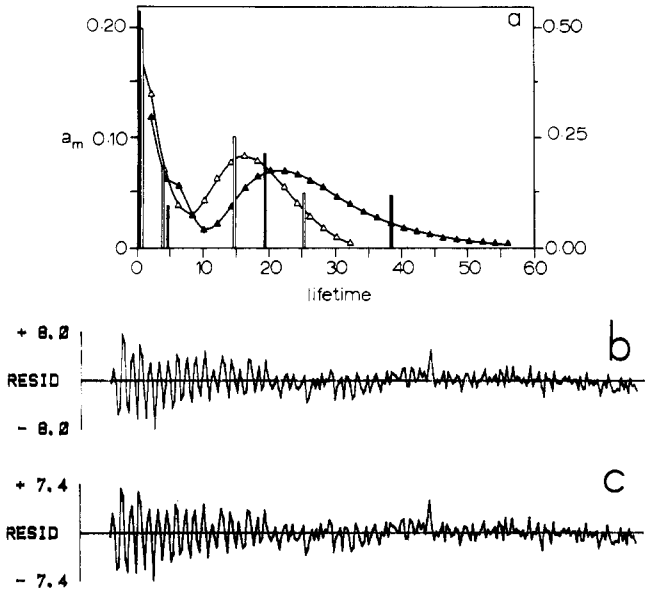

FIGURE 2: Recovered fluorescence decay parameters and lifetime distributions (a) for *cis*- (open symbols) and *trans*- (solid symbols) parinaric acids in DMPC vesicles at 15 °C. The height of the bar represents the value of the preexponential at that lifetime referenced to the right-hand axis. The decay parameters for *cis*-parinaric acid are the same as in Figure 1. The values for *trans*-parinaric acid are $a_1 = 0.58$, $\tau_1 = 0.30$ ns; $a_2 = 0.10$, $\tau_2 = 4.63$ ns; $a_3 = 0.21$, $\tau_3 = 19.7$ ns; $a_4 = 0.18$, $\tau_4 = 38.1$ ns; and $\chi^2 = 6.35$. The lifetime distributions recovered by the exponential series method are referenced to the left-hand axis. Uncertainties in the numbers quoted are in the last digit. Comparison of the weighted residuals for the *cis*-parinaric acid data in (a). The residuals are for fits at 2×10^5 CPC (b) to four exponentials (see Figure 1d) and (c) to the exponential series method. The latter pattern is more random and the spread is less, but the small differences are not sufficient to establish unequivocably which is the better fit by visual inspection. As discussed in the text, other methods are necessary.

If discrete lifetimes with separations as large as those estimated by the multiexponential method were in fact real, then they would be correctly recovered by the exponential series method. This point is illustrated in Figure 3a, which shows the results of both a multiexponential fit and an exponential series fit to composite 3-methylindole decay data. The composite decay was the sum of three experimental single-exponential decay curves with the lifetimes indicated. These data are real and include all sources of potential artifacts such as RF noise. Although the fit tends to overestimate the lifetimes, the three lifetimes are clearly resolved. Note that the data in Figure 3a correspond to the worst case, i.e., narrowest distribution, observed in any of the parinaric acid experiments. Conversely, when the exponential series method recovers a distribution of lifetimes, this distribution is an accurate representation of the true distribution. This is illustrated in Figure 3b by utilizing computer-generated data. The continuous distribution is represented as the sum of 112 discrete lifetimes. The distribution recovered in the exponential series fit matches the true distribution over the entire lifetime range including the spike at short lifetimes. The deviations of the fit from the input data are typical of many distributions examined in this way. At this stage of development we feel these levels of deviations are more than satisfactory. Note that this simulation corresponds to the broadest distribution which, by virtue of the number of parameters, is the hardest to fit. In view of these results, we conclude that the data in Figure 2 for parinaric acid are correctly described by a continuous distribution. Clearly the four lifetimes recovered by the multiexponential method offer very little insight into the shape of the underlying distribution, and it would be erroneous in this case to interpret these lifetimes as arising from discrete emitting states or species in this system.

Figure 4 presents the distributions of lifetimes arising from analyses of fluorescence decay curves for the trans (Figure 4a) and cis (Figure 4b) isomers in DMPC vesicles at several temperatures in the range from 22.4 to 24.5 °C. This range brackets the main phase transition temperature for this lipid at ~23.5 °C. It is evident for both systems that, at the lower temperatures, the lifetime distribution is broad and peaked at long lifetimes (10 ns for cis and 11 ns for trans). At the higher temperatures the distribution is narrower and centered at a smaller lifetime (6 ns for cis and 7 ns for trans). At the intermediate temperature (within the phase transition), the distribution is featureless and resembles a poorly resolved mixture of the high- and low-temperature distributions.

Recently Parasassi et al. (1984) showed that the parinaric acids exhibit multiexponential decay in homogeneous solution as well as in membranes. At ambient temperatures, better than 90% of the emission is associated with a single lifetime of about 1–2 ns. We have repeated these measurements in ethanol, cyclohexanol, and glycerol at 23 °C and find by normal multiple-exponential fitting methods essentially the

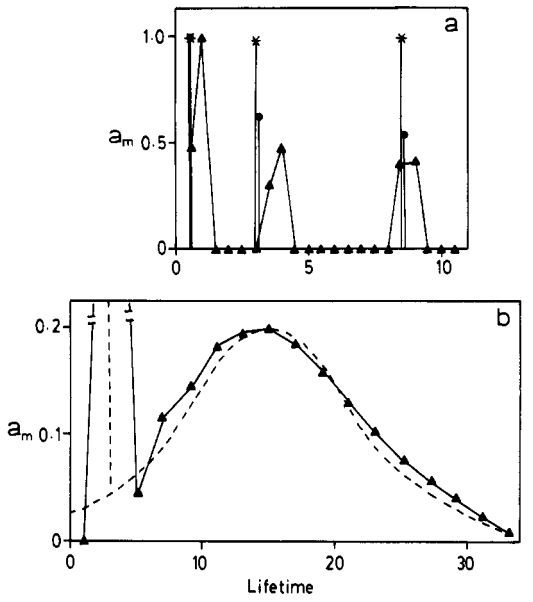

FIGURE 3: Comparison of fitting multiexponential and exponential series methods to known distributions. (a) Real data composed of fluorescence decay signals from 3-methylindole solutions quenched at different pHs and summed. The three lifetimes (*) are at 0.48, 3.03, and 8.52 ns. The multiexponential fitting recovers the three lifetimes very well (●), although their relative preexponentials are skewed ($a_1 = 0.47 \pm 0.007$, $\tau_1 = 0.52 \pm 0.01$; $a_2 = 0.28 \pm 0.002$, $\tau_2 = 3.14 \pm 0.03$; $a_3 = 0.25 \pm 0.002$, $\tau_3 = 8.63 \pm 0.02$; $\chi^2 = 2.49$). The exponential series method likewise recovers the three individual lifetimes (▲), although the short lifetimes are shifted slightly to the high side. Note that the lifetimes chosen correspond closely to those recovered for *cis*-parinaric acid in membranes at high temperatures. (b) Simulated data (---) for the sum of a single lifetime at 3 ns and a Gaussian distribution of lifetimes centered at 15 ns with a standard deviation of 7.5 ns. The input data contained a preexponential for the short lifetime 20-fold greater than that of the 15-ns lifetime. Clearly the exponential series method (▲) recovers the shape of the distribution extremely well, although the amplitude of the spike is only about half that expected. Uncertainties in the numbers quoted are in the last digit.

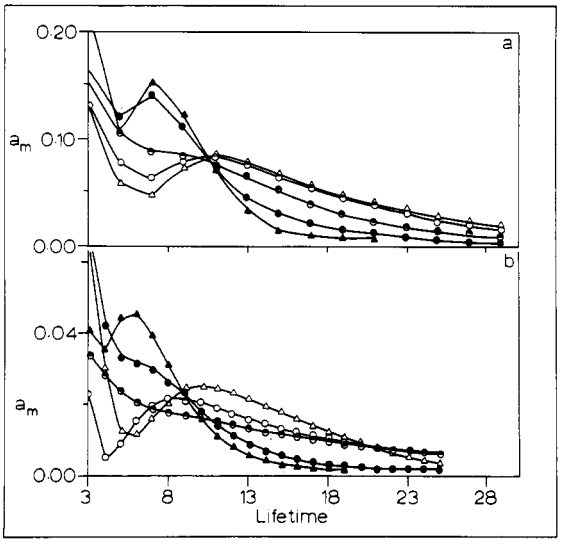

FIGURE 4: Fluorescence lifetime distributions as a function of temperature for (a) *trans*-parinaric acid and (b) *cis*-parinaric acid in DMPC vesicles: (a) △, at 22.8 °C; ○, at 23.3 °C; ◒, at 23.6 °C; ●, at 24.0 °C; ▲, at 24.5 °C; (b) △, at 22.5 °C; ○, at 23.0 °C; ◒, at 23.5 °C; ●, at 23.9 °C, ▲, at 24.4 °C. Note the invariant point at 10.5 ns for trans and at 9 ns for cis. The mid-temperature curves are poorly resolved and hard to fit, which is causing the poor scaling for the cis data at 23.5 °C [◒ in (b)].

same results. The exponential series method of analysis, however, shows that while 95% of the emission occurs with an average lifetime of 1.3 ns, there is in fact a narrow distribution of lifetimes ranging from 1 to 2 ns. There is therefore no conflict in interpretation between our solution results and those in membranes. In both cases a distribution of lifetimes appears to describe the emission decay correctly.

It is interesting to note that at one particular lifetime the preexponential factor is insensitive to temperature. This is most clearly seen in the trans data and is analogous to a spectroscopic isosbestic point. An invariant point like this will arise whenever two distributions interconvert if the observable is additive and proportional to the population. In the present case, the distributions are normalized probabilities that an excited molecule can decay at a particular lifetime, and they should satisfy these criteria. Figure 4, therefore, provides evidence that as the membrane changes from the pure gel to the pure liquid-crystalline state as the temperature is increased, one lifetime distribution converts *quantitatively* into another. This is to be expected at the phase transition if a single physical process is responsible for the lifetime being distributed, but it is inconsistent with the concept that long- and short-lifetime components behave differently at the transition (Wolber & Hudson, 1981; Gallay & Vincent, 1986).

Although not shown in Figure 4, there is a significant contribution to the lifetime distribution at short lifetimes (Figure 2). This feature is not typical of the parinaric acids (Wolber & Hudson, 1981) and does not appear to vary with temperature. We believe that this short-lifetime component might arise from a contaminant in the lipid, since we have observed similar emission from pure lipid samples. This conclusion is further supported by the observation that the short-lifetime contribution is proportionally larger for the cis than for the trans isomer, as expected since the former has a smaller quantum yield. (The RF artifact will also increase the uncertainty at short lifetimes.) Whatever the source, the "contaminant" plus RF does not cause any significant problems for recovering the distribution of lifetimes at longer times.

The lifetime distributions in Figure 4 are represented by the preexponential factor at each lifetime and are normalized to unit area. This is a fundamentally important distribution since it shows the fraction of the initially excited population that decays at a particular lifetime. It should be noted that for independent emitters the preexponential is a product of the radiative lifetime and the initial excited-state population of a species. Assuming that the radiative lifetime is the same for all members of the distribution and that the radiative lifetime does not change as the distribution changes, the distributions shown reflect the fractional populations in the excited state. The former assumption is reasonable if the distribution arises from different efficiencies of nonradiative decay paths, while the latter assumption is almost certainly true for the narrow temperature range shown in Figure 4. The exact source of a distribution in nonradiative decay paths is unknown, but it is possible that either different orientations within the bilayer, different exposure to hydration in the bilayer, or different degrees of freedom of rotational flexibility play a role.

Once the distributions have been established, it is possible, and informative, to calculate the corresponding distributions of lifetimes representing the relative emission intensity at each lifetime. These are obtained by calculating, for each lifetime, the relative quantum yield:

$$\phi_m^r = a_m\tau_m / \sum a_m\tau_m \qquad (3)$$

The quantity ϕ_m^r is equal to the fraction of photons emitted with lifetime τ_m under long-term and continuous illumination conditions, corresponding to the integration of eq 1 over long

Table I: Fluorescence Lifetime Comparisons

(A) Mean Lifetimes from Different Fits for *trans*-Parinaric Acid at 15 °C in DMPC

CPC	$\langle\tau\rangle^a$ (ns) $N^b = 2$	$N^b = 3$	$N^b = 4$	ESM[c]
200 000	27.5	27.8	27.6	28.1
50 000	27.7	27.8	28.0	NA
20 000	28.2	28.6	28.7	NA

(B) Recovered and Mean Lifetimes for Selected Probes

probe	lipid	t (°C)	$\tau_1(a_1)^d$	$\tau_2(a_2)^d$	$\tau_3(a_3)^d$	$\langle\tau\rangle^a$ (ns)	ref
t-PnA	DMPC	22.3	2.3 (0.30)	12.5 (0.47)	29.5 (0.23)	20.5	*e*
t-PnA	DMPC	24.5	2.2 (0.46)	8.7 (0.49)	26.3 (0.04)	10.7	*e*
c-PnA	DMPC	22.5	0.3 (0.36)	3.5 (0.28)	14.5 (0.37)	12.7	*e*
c-PnA	DMPC	24.4	0.4 (0.36)	3.0 (0.38)	9.7 (0.26)	7.4	*e*
nystatin	DMPC	20		17 (0.5)	33 (0.5)	25	*f*
nystatin	DMPC	32		1.6 (0.4)	7.4 (0.6)	5.1	*f*
2-AS	POPC	−10		5.1 (0.48)	13.4 (0.52)	11.3	*g*
7-AS	POPC	−10		6.0 (0.39)	14.7 (0.61)	12.8	*g*
9-AS	POPC	−10		7.3 (0.42)	15.8 (0.58)	13.7	*g*
12-AS	POPC	−10		7.2 (0.42)	16.9 (0.58)	14.6	*g*

[a] The mean lifetime as defined in eq 4. [b] N refers to the number of exponentials in eq 1. [c] Exponential series method. NA = not applicable. [d] Preexponentials for the parinaric acid data but relative quantum yields (eq 3) for the other data. [e] This work. [f] Petersen et al. (1987). [g] Vincent and Gallay (1984).

times. Examples of the resulting distributions are shown in Figure 5a at two temperatures for *cis*-parinaric acid. These distributions are relevant for comparison with steady-state quantum yield measurements. The mean of each distribution, indicated by the vertical arrowheads, correspond exactly to the quantum yield weighted average lifetime $\langle\tau\rangle$:

$$\langle\tau\rangle = \sum a_m\tau_m^2/\sum a_m\tau_m = \sum \phi_m^r\tau_m \qquad (4)$$

It is important to note that the lifetimes recovered by any of the fitting methods employed distribute such that the moments of the distribution remain constant. In particular, as illustrated in Table IA, the mean lifetime is the same whether calculated from two, three, or four exponential fits or from the complete distributions, and they are quite accurately determined by two or three exponential fits of data accumulated at low levels of precision. Although this clearly shows that it is possible to calculate a "mean" lifetime from less precise data, the physical meaning of such a value is not apparent unless the underlying distribution is known. Moreover, comparisons of changes in mean lifetimes implicitly assume that the shape of the distribution remains the same. To test this, it is useful to scale the distributions to unit intensity at unit lifetime simply by dividing all values by the value at the peak of the distribution. Examples of these dimensionless distributions are shown in Figure 5b,c. In this particular system, there is very little difference between the cis and trans isomers (Figure 5b), and there is very little change at higher temperatures (Figure 5c). The distributions of lifetimes need not be symmetrical since the actual physical process is more likely to cause a normal distribution in nonradiative rate constants. This point needs further investigation. Nevertheless, the scaled distributions recovered are remarkably constant, and this lends some credence to comparisons of average parameters for these particular probes. Since it is always possible to calculate the mean parameters once the distribution is known, while it is impossible to extract the distribution from the mean values, it is clearly important to determine the distribution for each case by careful analysis of high-precision data.

The observations that the lifetime distributions interconvert in the narrow temperature range shown in Figure 4 and that they scale to the same distribution in the range from 15 to 30 °C as shown in Figure 5 are suggestive of a single homogeneous distribution. Nevertheless, the current data analyses do not provide the resolution necessary to conclude unambiguously that only a single distribution is present. It is quite possible that the broad distribution, particularly at low temperatures, is in fact a superposition of two or more distributions.

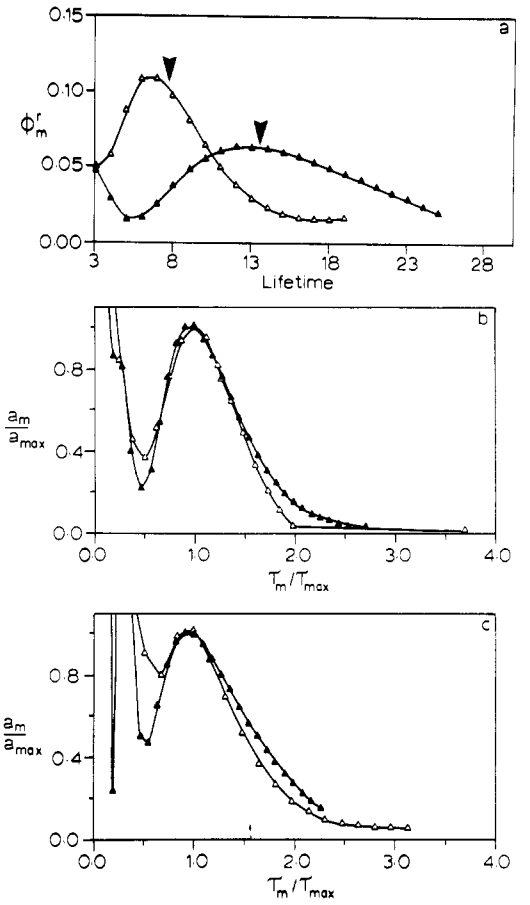

FIGURE 5: (a) Relative quantum yield distribution as a function of temperature for *cis*-parinaric acid in DMPC vesicles: △, at 24.4 °C; ▲, at 22.5 °C. The average lifetimes calculated from the results of the four-exponential and the exponential series fitting methods are identical and are shown by the arrowhead. (b) Distributions of lifetimes scaled by the maximal preexponential, a_{max}, and the corresponding lifetime, τ_{max}, for *cis*- (△) and *trans*- (▲) parinaric acid at 15 °C. These scaled distributions are virtually superimposable. (c) Distributions of lifetime scaled as in (b) of the high- and low-temperature data shown in (a) for *cis*-parinaric acid. These are superimposable on those in (b), showing the lack of temperature dependence from 15 to 24.4 °C.

It is important to question the implication of having a distribution of lifetimes rather than a set of discrete values. From a physical perspective, particularly in membranes, it is easier to rationalize continuous distributions than to explain singular heterogeneities, i.e., specific regions of unique behavior. In this sense, the distribution analysis is a simplification. In the particular cases where the scaled distribution does not change with temperature, phase change, or other perturbations, the mean parameters are still useful measures of the dynamics of the membrane. For example, it is clear for the parinaric acids discussed here that the quantum yield of emission measured in steady-state experiments is directly proportional to the mean lifetime calculated from the distributions (e.g., at 22.5 °C $\phi_F = 0.26$ and $\tau_0 = 13$ ns, while at 24.5 °C $\phi_F = 0.14$ and $\tau_0 = 7.5$ ns). Moreover, the radiative lifetime calculated for the parinaric acid probes in membranes from the average lifetime ($\tau_F = 50$–90 ns) is comparable to those estimated in a variety of organic solvents ($\tau_F = 60$–100 ns) (Sklar et al., 1977). However, for these comparisons to make sense, it is imperative for one to know that the fundamental lifetime distribution maintains the same shape.

When a fluorescence decay contains contributions from anisotropy, the intensity decay can be described by

$$D(t) = [\sum_{m}^{N} a_m \exp(-t/\tau_m)][\sum_{l}^{P} b_l \exp(-t/\phi_l)] = S_1(t)S_2(t) \quad (5)$$

provided the emission arises from a single emitting or rotating species (Chen et al., 1977; Ross et al., 1981). Otherwise, the difference decay is a complicated average. As long as the lifetime distribution process applies equally to each component of the anisotropy distribution process, they are uncorrelated and eq 5 would remain valid, and the lifetime $[S_1(t)]$ and anisotropy $[S_2(t)]$ contributions to the decay should act independently. The specific form of the lifetime decay signal would then become irrelevant, since its contribution will cancel in the anisotropy calculation. Nevertheless, analysis of $D(t)$ to recover $S_2(t)$ usually requires a good estimate of $S_1(t)$ in order to avoid deconvolution problems. In fact, only a reasonably good fit to the data at the level of the precision available is needed to obtain a satisfactory value of $S_2(t)$. It is, in principle, possible to apply the exponential series analysis method to the anisotropy decay as well as to the lifetime decay. This could reveal a distribution of rotational correlation times. It may be instructive to analyze more carefully the exact implications of distributions of lifetimes and correlation times on the interpretation of both steady-state and time-resolved anisotropy measurements.

The data presented here provide clear evidence that, for parinaric acids dissolved in phospholipid bilayer membranes, the fluorescence decay data are best analyzed and interpreted in terms of a continuous distribution of lifetimes, rather than as a sum of a few discrete lifetimes. The characteristic features of the two and three exponential fits applied to lower precision fluorescence decay data from parinaric acids include the extraction of lifetimes that differ only by a factor of 2 or 3 and estimates of preexponential factors that vary smoothly as the temperature is changed. These features are common to many membrane probes, a few of which are listed in Table IB along with previously determined lifetime values. Because of the similarity with parinaric acids, we predict that all of the probes listed will exhibit fluorescence decays which reflect continuous, unimodal distributions of decay times. Whether these distributions behave as nicely as those for the parinaric acids remains to be established. In the meantime, the interpretation of changes in the lifetimes estimated by two or three exponential fits must be approached with considerable caution.

References

Blatt, E., & Sawyer, W. H. (1985) *Biochim. Biophys. Acta 822*, 43.

Chen, L. A., Dale, R. E., Roth, S., & Brand, L. (1977) *J. Biol. Chem. 252*, 2163.

Devaux, P. F., & Seigneuret, M. (1985) *Biochim. Biophys. Acta 822*, 63.

Fung, B. K.-K., & Stryer, L. (1978) *Biochemistry 17*, 5341.

Gallay, J., & Vincent, M. (1986) *Biochemistry 25*, 2650.

James, D. R., & Ware, W. R. (1985) *Chem. Phys. Lett. 120*, 450.

James, D. R., & Ware, W. R. (1986) *Chem. Phys. Lett. 126*, 7.

Karnovsky, M. J., Kleinfeld, A. M., Hoover, R. L., & Klausner, R. D. (1982) *J. Cell Biol. 97*, 73.

Kawato, S., Kinosita, K., Jr., & Ikegami, A. (1977) *Biochemistry 16*, 2319.

Klausner, R. D., Kleinfeld, A. M., Hoover, R. L., & Karnovsky, M. J. (1980) *J. Biol. Chem. 255*, 1286.

Lakowicz, J. R., Cherek, H., Maliwal, B. P., & Gratton, E. (1985) *Biochemistry 24*, 376.

Parasassi, T., Conti, F., & Gratton, E. (1984) *Biochemistry 23*, 5660.

Petersen, N. O., Gratton, R. B., & Pisters, E. M. (1987) *Can. J. Chem. 65*, 238.

Ross, J. B. A., Schmidt, C., & Brand, L. (1981) *Biochemistry 20*, 4369.

Sklar, L. A., Hudson, B. S., Petersen, M., & Diamond, J. (1977) *Biochemistry 16*, 813.

Vincent, M., & Gallay, J. (1984) *Biochemistry 23*, 6514.

Ware, W. R., Pratinidhi, M., & Bauer, R. K. (1983) *Rev. Sci. Instrum. 54*, 1148.

Wolber, P. K., & Hudson, B. S. (1981) *Biochemistry 20*, 2800.

Yguerabide, J., & Foster, M. C. (1981) *Mol. Biol., Biochem. Biophys. 31*, 199.